View Online / Journal Homepage / Table of Contents for this issue
Dynamic Article Links

Nanoscale

Cite this: *Nanoscale*, 2012, **4**, 3410

www.rsc.org/nanoscale

PAPER

Flexible and mechanical strain resistant large area SERS active substrates

J. P. Singh,*[ab] HsiaoYun Chu,[c] Justin Abell,[d] Ralph A. Tripp[a] and Yiping Zhao[c]

Received 3rd January 2012, Accepted 21st March 2012
DOI: 10.1039/c2nr00020b

We report a cost effective and facile way to synthesize flexible, uniform, and large area surface enhanced Raman scattering (SERS) substrates using an oblique angle deposition (OAD) technique. The flexible SERS substrates consist of 1 μm long, tilted silver nanocolumnar films deposited on flexible polydimethylsiloxane (PDMS) and polyethylene terephthalate (PET) sheets using OAD. The SERS enhancement activity of these flexible substrates was determined using 10^{-5} M *trans*-1,2-bis(4-pyridyl) ethylene (BPE) Raman probe molecules. The *in situ* SERS measurements on these flexible substrates under mechanical (tensile/bending) strain conditions were performed. Our results show that flexible SERS substrates can withstand a tensile strain (ε) value as high as 30% without losing SERS performance, whereas the similar bending strain decreases the SERS performance by about 13%. A cyclic tensile loading test on flexible PDMS SERS substrates at a pre-specified tensile strain (ε) value of 10% shows that the SERS intensity remains almost constant for more than 100 cycles. These disposable and flexible SERS substrates can be integrated with biological substances and offer a novel and practical method to facilitate biosensing applications.

Introduction

Surface-enhanced Raman scattering (SERS) has been recognized as a highly sensitive and label free analytical tool to observe trace amounts of chemical and biological molecules.[1–3] SERS offers an enormous enhancement ($\sim 10^{10}$ times) over traditional Raman signal intensity, a feature that has made this technique ultra-sensitive for successful detection of trace substances and even for a single molecule.[4] Substantial literature exists in the area of fabrication of SERS substrates,[5–27] but few methods are available to develop a uniform, reproducible, robust, stable, and cost-effective SERS substrate. Most of these fabrication methods focus on achieving large enhancement factors, but fail to perform in a reproducible and cost-effective manner and generally lack requisite characteristics needed to move SERS to a platform enabling technology. We have recently shown that oblique angle deposition (OAD) can be used to prepare aligned silver nanorod (AgNR) arrays having a large ($\sim 10^8$) SERS enhancement factor.[28–32] OAD is based on a conventional physical vapor deposition principle and can be used to fabricate aligned and tilted Ag nanorod arrays on large substrate areas. This method involves positioning the substrate at a specific angle such that the vapor from the source is incident on the substrate at a glancing angle (>75°). This process produces a geometric shadowing effect that results in the preferential growth of nanorods on the substrate towards the direction of deposition. Silver nanorod array substrates prepared by the OAD process have previously been shown to provide SERS enhancement factors of $\sim 10^8$.[30–32] The OAD technique offers an easy, straightforward, and inexpensive method for fabrication of silver nanorod arrays for high sensitivity SERS applications. SERS substrates produced by OAD have the added advantages of uniformity and reproducibility. We have previously reported less than 12% variability for point-to-point intra-substrate assessment, 6–13% for the inter-substrate assessment from a single fabrication batch, and less than 15% for inter-batch variability.[30,33]

Currently, silicon wafers and glass slides are two of the most common substrates for deposition of SERS active layers. However, these substrates are rigid and brittle. For some applications such as packaging or tracking, flexible SERS substrates would be more appropriate. Flexible substrates have advantages over the conventional rigid substrates in their flexibility to conform to the underlying object as they can be wrapped onto curved surfaces and can be easily cut into different shapes and sizes. To make flexible substrates effective requires chemical/thermal stability and compatibility with existing fabrication techniques, while remaining relatively low cost to fabricate. There have only been a few attempts to achieve flexible large area SERS substrates.[34–36] Recently, Chung *et al.*[34] have reported the fabrication of large area flexible SERS active substrates using a shadow mask assisted evaporation technique. This method has an advantage of being simple and different types of

[a]*Department of Infectious Diseases, Nanoscale Science and Engineering Center, University of Georgia, Athens, GA 30602, USA*
[b]*Physics Department, Indian Institute of Technology Delhi, Hauz Khas, New Delhi 110016, India. E-mail: jpsingh@physics.iitd.ac.in*
[c]*Department of Physics and Astronomy, Nanoscale Science and Engineering Center, University of Georgia, Athens, GA 30602, USA*
[d]*Department of Biological and Agricultural Engineering, University of Georgia, Athens, GA 30602, USA*

nanostructure morphology such as nano-pillar, nano-nib, and nano-cylinder can be fabricated on a large area. Despite its advantage, the method suffers from being a multi-step process involving metal evaporation onto an anodized alumina oxide (AAO) nanoporous membrane, dissolution of the AAO template in NaOH solution and then settlement of the metallic nanostructure film onto the polydimethylsiloxane (PDMS) substrate. Although the largest SERS signal enhancement was observed for nano-tip morphology, the most reproducible SERS signal was observed from the nano-pillar arrays structure which resembles our OAD grown Ag nanorod arrays morphology. In further interesting research, Lee and researchers[35] have reported SERS substrates based on flexible filter paper scaffolding. These SERS substrates have advantages of being biodegradable and having the ability to easily absorb the fluids. But, optimization of homogeneity of the SERS signal over these paper substrates is still a matter of research. Currently, there are no reports on the performance of flexible SERS substrates under mechanical strain conditions, which is needed before any practical applications of these flexible SERRS substrates can be realized.

Here, we report the fabrication and characterization of OAD-deposited AgNR arrays on free-standing PDMS and polyethylene terephthalate (PET) sheets as flexible SERS substrates. These SERS substrates exhibit comparatively similar SERS enhancement to their glass substrate counterparts. The *in situ* SERS measurements over these flexible substrates under mechanical strain conditions show that the SERS signal intensity remains almost constant for an induced tensile strain value as high as 30%. These flexible SERS substrates were also assessed for cyclic tensile and bending strains and found to be functional as SERS-active substrates. Flexible SERS substrates may find potential applications in routine SERS detection applications that include practical pathogen identification, packaging, and tracking processes.

Materials and methods

Fabrication of flexible SERS substrates

The SERS-active AgNR arrays were fabricated by the OAD technique using a custom-designed electron beam evaporation (E-beam) system. The PDMS films (~1 mm thickness) were prepared by mixing a pre-polymer (Slygard 184 from Dow Corning) with a curing agent in a 10 : 1 ratio at room temperature, the mixture was then poured on a pre-cleaned Si substrate, and was cured for 1 hour at a temperature of 70 °C. PET sheets (DuPont Teijin Films, Hopewell, VA) were cleaned with commercial detergent and deionized water. For deposition of AgNR arrays, PET and PDMS sheets were cut into 20 mm × 40 mm size. For the tensile test, the PDMS substrate was mounted on a tensile tester and the PET substrate was directly attached to the substrate holder by a double-sided tape. The substrates were dried with a stream of nitrogen gas before loading into the E-beam evaporation chamber. The source material for evaporation was Ti pellets (Kurt J. Lesker, Clariton, PA, 99.995%) and Ag pellets (Kurt J. Lesker, Clariton, PA, 99.999%). During fabrication, the film thickness was monitored by a quartz crystal microbalance (QCM) positioned at normal incidence to the vapor source direction and the deposition pressure was ~1 × 10^{-6} Torr. Base layers of Ti (20 nm) and silver (200 nm) films were first evaporated onto the substrates at a normal angle to the substrate surface at a rate of 0.2 nm s^{-1} and 0.3 nm s^{-1}, respectively. The substrates were then rotated to 86° with respect to the vapor incident direction and Ag nanorods were grown at this oblique angle by depositing another 2000 nm of Ag (as reported by the QCM) with a deposition rate of 0.3 nm s^{-1}.

SERS characterization

The SERS spectra from flexible substrates were acquired using a HRC-10HT Raman Analyzer system (Enwave Optronics Inc., Irvine, CA). The excitation source was a near-infrared diode laser with a wavelength of $\lambda = 785$ nm. The unpolarized excitation laser beam coupled to a 100 μm fiber was focused onto the substrate through the Raman probe head. The focal length of the Raman probe was ~7 mm and the diameter of the laser spot was 0.1 mm. The laser power at the sample was 30 mW and the spectral collection time was 10 s. The molecular probe used in this study was *trans*-1,2-bis(4-pyridyl) ethylene (BPE, 99.9+%, Sigma). BPE solutions were prepared by sequential dilution in ACS grade methanol (Fisher Scientific). A 2 μL droplet of 10^{-5} M BPE solution was applied onto the AgNR substrate and allowed to dry before the acquisition of data. SERS spectra were collected from multiple points across the BPE-treated portion of the AgNR film.

Tensile and bending tests

The SERS performances of the flexible AgNR PDMS and PET substrates were analyzed *in situ* as a function of mechanical strain (tensile test for PDMS and bending test for PET substrates) and for different loading cycles. SERS spectra of AgNR on flexible PDMS and PET substrates were initially measured in their relaxed and unbent position. The PDMS substrate was held in place during the tensile experiments by two posts mounted on an optical rail. Tensile experiments were performed by moving the posts farther away from each other while monitoring the SERS spectra. The bending tests on PET substrates were performed in a similar way by holding the substrate on the two posts mounted on the optical rail and moving them close to each other. The schematic of the setup is shown in Fig. 1. The figure shows two posts mounted on the optical rails. The separation between the posts can be linearly changed by tightening/un-tightening the screw attached to one of the posts for tensile and bending experiments as shown in Fig. 1(a) and (b), respectively. Fig. 1(c) shows a photograph of the AgNR–PET SERS substrate. These substrates were also tested for the effects of cyclic tensile and bending effects on the SERS spectra. For cyclic tensile loading, the PDMS substrate was tested for a pre-specified 10% tensile

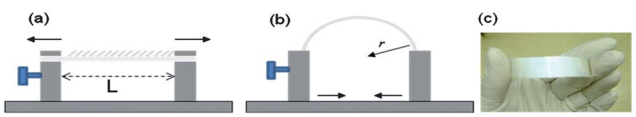

Fig. 1 Schematic diagram showing (a) tensile loading and (b) bending of the flexible AgNR–PDMS/PET SERS substrates, and (c) photograph of a AgNR–PET SERS substrate.

strain (ε). A complete bending cycle consists of continuously bending the substrate with incremental decreases in the radius of curvature, then exactly reversing the process.

Results and discussion

Surface enhanced Raman scattering of flexible substrates

To characterize the SERS response of the flexible substrates, Raman spectra of BPE were collected by spreading 2 μL of a 10^{-5} M BPE solution in methanol on the film surface. The averaged SERS spectra of BPE on the AgNR arrays deposited on PET and PDMS substrates are shown in Fig. 2(a). The main bands of BPE at around 1015, 1200, 1610 and 1640 cm^{-1} can be assigned to the pyridine ring breathing, ethylenic C=C in-plane ring mode, aromatic ring stretching mode, and the C=C stretching mode, respectively.[37] The baseline-corrected peak height of the BPE peak located at about 1200 cm^{-1} was used to quantify the overall SERS response, and is denoted as I_{1200}. The SERS response of the AgNR arrays deposited on PET and PDMS substrates was found to be comparable to that deposited on a conventional glass substrate. The background SERS spectra of bare AgNR arrays deposited on PET and PDMS substrates before any analyte molecules were applied on the substrate are shown in Fig. 2(b). Several small peaks can be seen in the background spectra at around 490, 690, and 1400 cm^{-1}. The broad peak around 1400 cm^{-1} could be attributed to amorphous carbon. Vapor deposited silver films and electrochemically reduced silver electrodes have been reported to exhibit backgrounds due to graphitic carbonaceous adsorption onto the substrate. The other bands in the spectra possibly arise from organic impurities from the ambient environment or out-gassing from the deposition chamber.

Effect of tensile strains on the SERS performance of AgNR–PDMS substrates

For the substrate to be an effective sensor, the flexible substrate must retain superior SERS performance during the mechanical deformation. The *in situ* SERS measurements were performed on AgNR arrays on flexible PDMS substrates under tensile strains. The tensile tests were performed by moving the mount post with respect to the stationary post and measuring the increment in the film length. The tensile strain (ε) is defined as the ratio of increase in the film length (ΔL) to its original unstrained film length (L). The SERS response of AgNR arrays on flexible PDMS substrate as a function of tensile strain is shown in Fig. 3(a). Here, the SERS response is plotted as the intensity of a 1200 cm^{-1} (I_{1200}) Raman peak of BPE as a function of tensile strain (ε). It is important to note that the Raman intensity remains almost constant with a maximum decrease of less than 10% at tensile strain (ε) value as high as 27%.

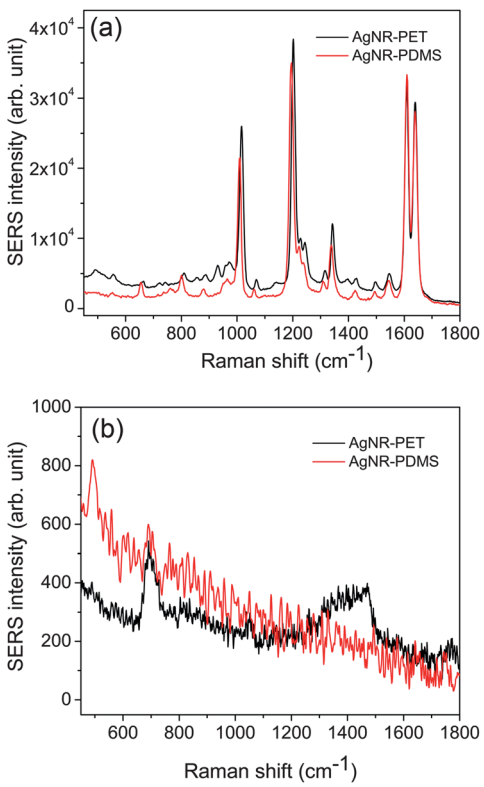

Fig. 2 (a) SERS spectra of BPE applied to AgNR arrays deposited on flexible PDMS and PET substrates. The spectra are the average of five different positions measured on each of the sample surfaces. (b) The background SERS spectra of bare AgNR arrays deposited on PDMS and PET substrates.

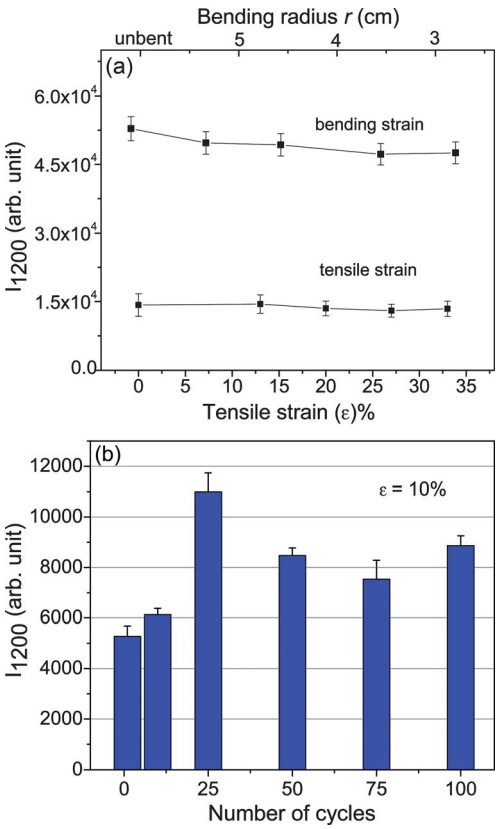

Fig. 3 (a) Plots of I_{1200} as a function of induced tensile strain (ε) in a flexible AgNR–PDMS SERS substrate. The variation of I_{1200} with bending radius r for a AgNR–PET SERS substrate is also shown in the same figure. (b) Bar graph showing the dependence of I_{1200} on the number of tensile loading cycles for a pre-defined 10% tensile strain.

Effect of bending strains on the SERS performance of AgNR–PET substrates

Similar *in situ* SERS measurements were also performed on AgNR arrays on flexible PET substrates under bending strains. The bending tests were performed by moving the mount post with respect to the stationary post and measuring the incremental decreases in the radius of curvature. Fig. 3(a) also shows the variation of I_{1200} as a function of the bending radius r of AgNR films on a PET substrate. The AgNR arrays on a PET substrate demonstrate a decrease of about 13% in SERS intensity with increase in bending radius r. The results show that regardless of the direction of strain induced, convex or concave bending of the flexible AgNR arrays on PET SERS substrates at different radii does not significantly impact the sensing of BPE.

Effect of cyclic tensile/bending strains on the SERS performance of flexible substrates

An additional concern with a flexible sensor is its ability to withstand cyclic deformation. To investigate this, the SERS response of AgNR arrays on a flexible PDMS substrate was measured after each cycle of a pre-specified tensile strain (ε) value of 10%. Each cycle consists of producing 10% tensile strain in the film and then relaxing back it to the normal state. The SERS response of the flexible substrate was observed for more than 100 such cycles. Fig. 3(b) illustrates a bar graph of a cyclic tensile loading experiment showing the variation of SERS I_{1200} intensity of BPE as a function of the number of tensile cycles. Surprisingly, the SERS intensity does not decrease with the number of tensile loading cycles and even an increase in the SERS intensity was observed. This may be due to the stress induced buckling pattern formation on the PDMS surface[38] which may introduce hot-spots for local SERS enhancement. However, after several hundred tensile loading cycles wrinkles were visually apparent on the AgNR–PDMS surface but scanning electron microscopy (SEM) images in Fig. 4 (before and after one hundred tensile loading cycles) show that the AgNRs morphology remains almost undamaged. Thus, it is not surprising that the SERS intensity remained mostly unchanged. These flexible and disposable SERS substrates can detect trace analytes, as indicated in Fig. 5 which shows the SERS spectra of 10^{-5} M melamine deposited on a AgNR based flexible PDMS SERS substrate.

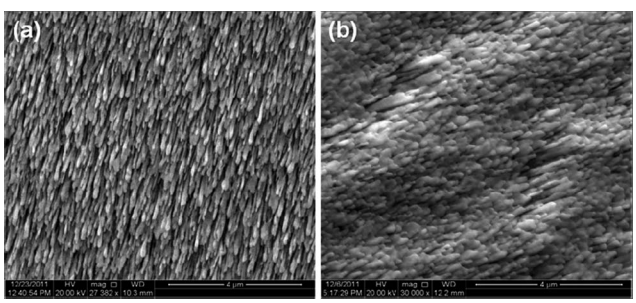

Fig. 4 SEM images of a flexible AgNR–PDMS substrate (a) before and (b) after one hundred tensile loading cycles.

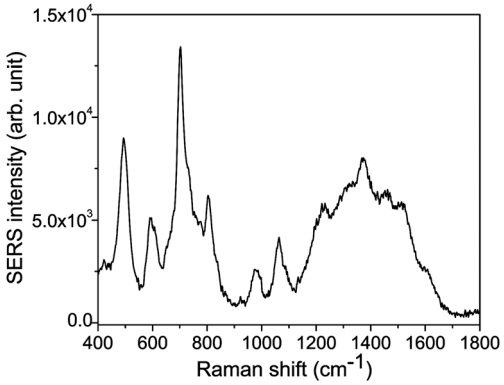

Fig. 5 SERS spectra of 10^{-5} M melamine applied to a flexible AgNR–PDMS SERS substrate.

The SERS responses to cyclic deformation of AgNR arrays on a flexible PET substrate with the induced curving strain are shown in Fig. 6. After the substrate was relaxed from the r = 2.8 cm bent position, the SERS response continued to decline by another 11% as the substrate was relaxed back to the unbent conformation; thus completing the first cycle and returning to the unbent configuration, the substrate retains 76% of the initial SERS intensity. The bending test was repeated for another cycle 2. Relaxing the substrate back to the unbent configuration and completing the second cycle, 57% of the initial SERS response was retained. The same substrate was then treated with further cyclic bending but this time in a convex manner. After convexly bending the flexible AgNR–PET substrate to r = 2.8 cm, 70% of SERS response was retained (relative to the I_{1200} *after* the concave bending cycles). The substrate response continued to decrease slightly after relaxing the substrate back to the unbent configuration, where it demonstrated 60% of the initial I_{1200}. Repeating the convex bending for cycle 2 and relaxing back to the unbent configuration, 53% of the initial SERS response was retained (relative to the I_{1200} *after* the concave bending cycles). These results demonstrate that although the cyclic bending has a significant effect on the SERS intensity, the SERS enhancement by AgNR arrays on flexible PET substrates is high enough to use it as an efficient flexible SERS sensor.

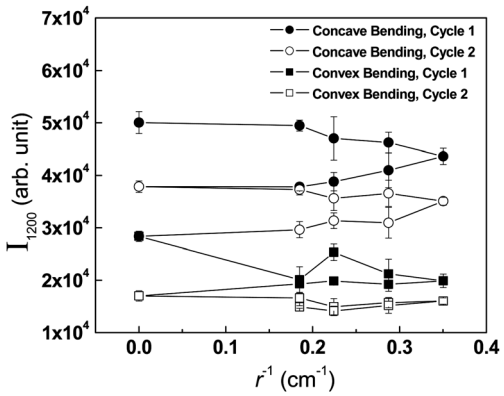

Fig. 6 Plots of I_{1200} *versus* radius of curvature (expressed as 1/radius) for cyclic concave and successive convex bending cycles for the same PET–AgNR SERS substrate.

Conclusions

In summary, we show that Ag nanorod arrays can be deposited on flexible PDMS and PET substrates to produce a comparable SERS response to those deposited on conventional glass slides. The AgNR arrays on these flexible substrates retain their SERS activity after undergoing repeated cyclic tensile and bending tests. The robustness of the AgNR-based PDMS and PET SERS substrates reveals possibilities for sensing with non-planar geometries in terms of flexible or wearable labels capable of monitoring biological and chemical agents. These flexible substrates offer a number of significant benefits over more conventional SERS substrates in that they are low-cost, flexible, mechanically robust and easy to pack, handle and discard after use to avoid cross-contamination.

Acknowledgements

PET plastic sheets were supplied by Prof. Howard Wang from SUNY-Binghamton. Both JA and YPZ are supported by USDA CSREES grant number 2009-35603-05001. This work was supported by ARL grant number W911NF-07-R-0001-04.

References

1 M. Fleischm, P. J. Hendra and A. McQuilla, *Chem. Phys. Lett.*, 1974, **26**, 163.
2 S. D. Hudson and G. Chumanov, *Anal. Bioanal. Chem.*, 2009, **394**, 679.
3 M. J. Natan, *Faraday Discuss.*, 2006, **132**, 321.
4 S. Nie and S. R. Emory, *Science*, 1997, **275**, 1102.
5 M. Kahl, E. Voges, S. Kostrewa, C. Viets and W. Hill, *Sens. Actuators, B*, 1998, **51**, 285.
6 M. A. De Jesus, K. S. Giesfeldt, J. M. Oran, N. A. Abu-Hatab, N. V. Lavrik and M. J. Sepaniak, *Appl. Spectrosc.*, 2005, **59**, 1501.
7 M. Sackmann, S. Bom, T. Balster and A. Materny, *J. Raman Spectrosc.*, 2007, **38**, 277.
8 L. Billot, M. L. de la Chapelle, A. S. Grimault, A. Vial, D. Barchiesi, J. L. Bijeon, P. M. Adam and P. Royer, *Chem. Phys. Lett.*, 2006, **422**, 303.
9 T. H. Reilly, J. D. Corbman and K. L. Rowlen, *Anal. Chem.*, 2007, **79**, 5078.
10 R. Alvarez-Puebla, B. Cui, J.-P. Bravo-Vasquez, T. Verse and H. Fenniri, *J. Phys. Chem. C*, 2007, **111**, 6720.
11 J. C. Hulteen, D. A. Treichel, M. T. Smith, M. L. Duval, T. R. Jensen and R. P. Van Duyne, *J. Phys. Chem. B*, 1999, **103**, 3854.
12 A. D. Ormonde, E. C. M. Hicks, J. Castillo and R. P. Van Duyne, *Langmuir*, 2004, **20**, 6927.
13 X. Zhang, C. R. Yonzon, M. A. Young, D. A. Stuart and R. P. Van Duyne, *IEE Proc.: Nanobiotechnol.*, 2005, **152**, 195.
14 C. L. Haynes, A. D. McFarland, M. T. Smith, J. C. Hulteen and R. P. Van Duyne, *J. Phys. Chem. B*, 2002, **106**, 1898.
15 G. Kartopu, M. Es-Souni, A. V. Sapelkin and D. Dunstan, *Phys. Status Solidi A*, 2006, **203**, R82.
16 L. S. Zhang, P. X. Zhang and Y. Fang, *J. Colloid Interface Sci.*, 2007, **311**, 502.
17 C. M. Ruan, G. Eres, W. Wang, Z. Y. Zhang and B. H. Gu, *Langmuir*, 2007, **23**, 5757.
18 B. L. Broglin, A. Andreu, N. Dhussa, J. A. Heath, J. Gerst, B. Dudley, D. Holland and M. El-Kouedi, *Langmuir*, 2007, **23**, 4563.
19 G. H. Gu, J. Kim, L. Kim and J. S. Suh, *J. Phys. Chem. C*, 2007, **111**, 7906.
20 I. Lombardi, P. L. Cavallotti, C. Carraro and R. Maboudian, *Sens. Actuators, B*, 2007, **125**, 353.
21 D. S. Jung, Y. M. Lee, Y. Lee, N. H. Kim, K. Kim and J. K. Lee, *J. Mater. Chem.*, 2006, **16**, 3145.
22 R. J. Walsh and G. Chumanov, *Appl. Spectrosc.*, 2001, **55**, 1695.
23 S. Chan, S. Kwon, T. W. Koo, L. P. Lee and A. A. Berlin, *Adv. Mater.*, 2003, **15**, 1595.
24 H. H. Lin, J. Mock, D. Smith, T. Gao and M. J. Sailor, *J. Phys. Chem. B*, 2004, **108**, 11654.
25 S. J. Henley, J. D. Carey and S. R. P. Silva, *Appl. Phys. Lett.*, 2006, **89**, 183120.
26 S. Chattopadhyay, H. C. Lo, C. H. Hsu, L. C. Chen and K. H. Chen, *Chem. Mater.*, 2005, **17**, 553.
27 M. Suzuki, W. Maekita, Y. Wada, K. Nakajima, K. Kimura, T. Fukuoka and Y. Mori, *Appl. Phys. Lett.*, 2006, **88**, 203121.
28 J.-G. Fan and Y.-P. Zhao, *Langmuir*, 2008, **24**, 14172.
29 J. L. Abell, J. D. Driskell, R. A. Dluhy, R. A. Tripp and Y. P. Zhao, *Biosens. Bioelectron.*, 2009, **24**, 3663.
30 S. B. Chaney, S. Shanmukh, R. A. Dluhy and Y. P. Zhao, *Appl. Phys. Lett.*, 2005, **87**, 031908.
31 J. D. Driskell, S. Shanmukh, Y. Liu, S. B. Chaney, X. J. Tang, Y. P. Zhao and R. A. Dluhy, *J. Phys. Chem. C*, 2008, **112**, 895.
32 Y.-J. Liu, H. Y. Chu and Y.-P. Zhao, *J. Phys. Chem. C*, 2010, **114**, 8176.
33 J. L. Abell, J. M. Garren and Y.-P. Zhao, *Appl. Spectrosc.*, 2011, **65**, 734–740.
34 A. J. Chung, Y. S. Huh and D. Erickson, *Nanoscale*, 2011, **3**, 2903.
35 C. H. Lee, M. E. Hankus, L. Tian, P. M. Pellegrino and S. Singamaneni, *Anal. Chem.*, 2011, **83**, 8953.
36 D. He, B. Hu, Q.-F. Yao, K. Wang and S.-H. Yu, *ACS Nano*, 2009, **3**, 3993.
37 C. E. Taylor, S. D. Garvey and J. E. Pemberton, *Anal. Chem.*, 1996, **68**, 2401.
38 W. T. S. Huck, N. Bowden, P. Onck, T. Pardoen, J. W. Hutchinson and G. M. Whitesides, *Langmuir*, 2000, **16**, 3497.

